Hindawi Publishing Corporation
Advances in Materials Science and Engineering
Volume 2012, Article ID 380306, 6 pages
doi:10.1155/2012/380306

Research Article

Size Effect on the Structural and Magnetic Properties of Nanosized Perovskite $LaFeO_3$ Prepared by Different Methods

Nguyen Thi Thuy[1] and Dang Le Minh[2]

[1] *Department of Physics, College of Education, Hue University, 34 Le Loi, Hue City, Vietnam*
[2] *Faculty of Physics, Hanoi University of Sciences, VNU, 334 Nguyen Trai, Thanh Xuan, Hanoi City, Vietnam*

Correspondence should be addressed to Nguyen Thi Thuy, nguyenthithuy0206@gmail.com

Received 24 April 2012; Accepted 19 June 2012

Academic Editor: David Cann

Nanosized $LaFeO_3$ material was prepared by 3 methods: high energy milling, citrate gel, and coprecipitation. The X-ray diffraction (XRD), differential scanning calorimetry (DSC), and thermogravimetric analysis (TGA) show that the orthorhombic $LaFeO_3$ phase was well formed at a low sintering temperature of 500°C in the citrate-gel and co-precipitation methods. Scanning electron microscope (SEM) and transmission electron microscope (TEM) observations indicate that the particle size of the $LaFeO_3$ powder varies from 10 nm to 50 nm depending on the preparation method. The magnetic properties through magnetization versus temperature $M(T)$ and magnetization verses magnetic field $M(H)$ characteristics show that the nano-$LaFeO_3$ exhibits a weak ferromagnetic behavior in the room temperature, and the $M(H)$ curves are well fitted by Langevin functions.

1. Introduction

The perovskite-type oxides (general, formula ABO_3, A, and B are the metallic ions) have been attracting much attention for more than two decades due to their potential commercial applications as catalysts for various reactions. Moreover, the modified perovskite compounds such as $La_{1-x}Sr_xMnO_3$, $La_{1-x}Pr_xMnO_3$, $La_{0.7}Sr_{0.3}Mn_{1-x}Ni_xO_3$, $Ca_{1-x}Nd_xMnO_3$, $CaMn_{1-x}Fe_xO_3$, and so forth [1–7] have received much attention because of their interesting physical effects: colossal magnetoresistance (CMR), giant magnetocaloric effect (GMCE), and high thermoelectric performance (TEP) at high temperature. In recent years, many laboratories in the world have studied $LaFeO_3$ as a thermoelectric material with high Seebeck coefficient and high power factor and it can be used as catalyst for methane combustion, the thin film gas sensors, and so forth. The $LaFeO_3$ thin film can be used as sensitive O_2 gas sensors [8] and nano-sized $LaFeO_3$ powder can be used as catalyst for the autoreforming of sulfur-containing fuels or for partial oxidation of methane (POM) to (H_2/CO) [9–12]. For preparation of those nanomaterials, various technological methods are used such as coprecipitation, sol-gel, hydrothermal reactions, mechanical alloying, pulsed wire discharge, shock wave, spray drying, and so forth.

In the present study, the nano-sized $LaFeO_3$ has been prepared by 3 methods: high energy milling, citrate gel, and co-precipitation. Beside determination of the particle size, crystalline, and microstructures, the magnetic properties were also investigated. The particle size of the samples prepared by different methods influenced strongly on the structural and magnetic properties of the material.

2. Experimental Procedure

The nano-$LaFeO_3$ was prepared using sol-gel, co-precipitation, and high-energy milling methods. These methods were performed as the following.

In the sol-gel method, the analytical grade $La(NO)_3 \cdot 6H_2O$, $Fe(NO_3)_3 \cdot 9H_2O$, and citric acid (CA) $C_6H_8O_7 \cdot H_2O$ were used as starting materials. The same mole equivalent amounts of metal nitrates were weighed according to the nominal composition $LaFeO_3$ and then dissolved in distilled water. The citric acid with the ratios (CA)/Σ(Metal ions) = (1.2–1.5) was then proportionally added to the metal nitrates solution. In the above ratio, (CA) and Σ(Metal ions)

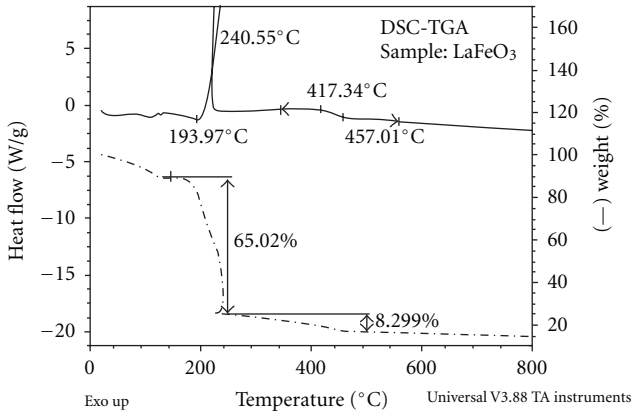

Figure 1: The DSC-TGA curves of the gel complex.

are concentration of (CA) and sum of concentration of metallic ions, respectively. The solution was concentrated by evaporation at 60–70°C with continuous stirring and pH controlled by NH_3 solution. The nanocrystals of perovskite $LaFeO_3$ were obtained by decomposition of the dried gel complex at selected temperatures: 300, 500, and 700°C in air.

In the co-precipitation method, $La(NO_3)\cdot 6H_2O$, $Fe(NO_3)_3\cdot 4H_2O$ were raw materials. NH_3 solution was added to the metal nitrates solution. The $La(OH)_3$ and $Fe(OH)_3$ were co-precipitated as hydroxide gel [13] at 80°C under continuous stirring and pH $\approx$ 10 to ensure the completely precipitation. Then, the hydroxide gel was filtered and dried. The dried powders were calcined at different temperatures ranging from 100 to 700°C for 3 h in air.

In the high-energy milling method, firstly, the bulk sample was prepared by ceramic method and then it was milled into the nanopowder using the high-energy milling equipment SPEX 8000D for 5 h.

Various techniques such as thermal analysis (DSC and TGA with SDT-2960-TA Instrument-USA.), XRD (Diffractometer D5005-Bruker), SEM (S-4800-Hitachi-Japan), and TEM (JEM1011-Jeol-Japan) were employed to characterize the nano-sized $LaFeO_3$ powder. The magnetic properties of the samples were examined by a vibrating sample magnetometer (VSM) DDS-880 (USA).

3. Results and Discussion

Figure 1 shows the DSC and TGA curves for the sample prepared by sol-gel method. It can be seen from Figure 1 that TGA curve exhibits a weight loss of about 65% corresponding to an exothermic peak in DSC curve at 240.55°C, those are the removal of the water from crystallization and decomposition process of the organic substances. Heating at higher temperature led to a small weight loss (~8.3%) at 250°C and finishing at 500°C associated with a peak at 457.01°C in the DSC curve. The weight loss (~65%) is due to the chemical changes as shown in the following equation [14]:

$$La(NO_3)_3\cdot 6H_2O + Fe(NO_3)\cdot 9H_2O + C_6H_8O_7\cdot H_2O \longrightarrow LaFeO_3 + 6CO_2 + 2N_2 + 2NO_2 + 20H_2O \quad (1)$$

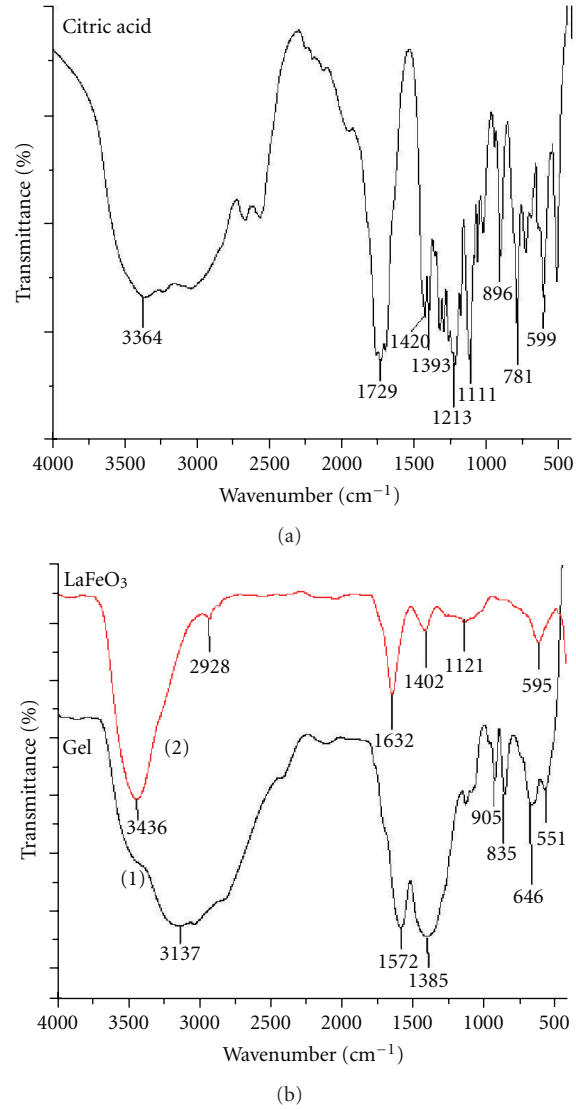

Figure 2: (a) FTIR spectra of citric acid; (b) FTIR spectra of gel complex (black line) and $LaFeO_3$ (red line).

During the evaporation of the solvent, a reddish-brown gas corresponding to NO_2 comes out of the solution. The above chemical formula only shows the result of chemical reaction but the nature of the sol-gel method is not pointed out. In the used sol-gel method, before creating the solid solution of $LaFeO_3$, the La and Fe ions have been presented in a gel complex. The Fourier transform infrared (FTIR) spectra of the citric acid, gel, and $LaFeO_3$ have been measured for demonstration of the process mentioned above [15].

The FTIR spectra of the citric acid, gel complex, and $LaFeO_3$ nanoparticles are shown in Figure 2. In Figure 2(b) (black line), two vibrational bands can be observed at 1572 cm^{-1} and 1385 cm^{-1} that are assigned to the stretching of C–O bonds. The bands occurred at 551 cm^{-1} and 646 cm^{-1} are corresponding to Fe–O and La–O bonds, respectively, and the wide band around 3137 cm^{-1} in Figure 2(b) (black-line) and 3364 cm^{-1} in Figure 2(a) correspond to the hydroxyl group. From the above spectroscopic observations

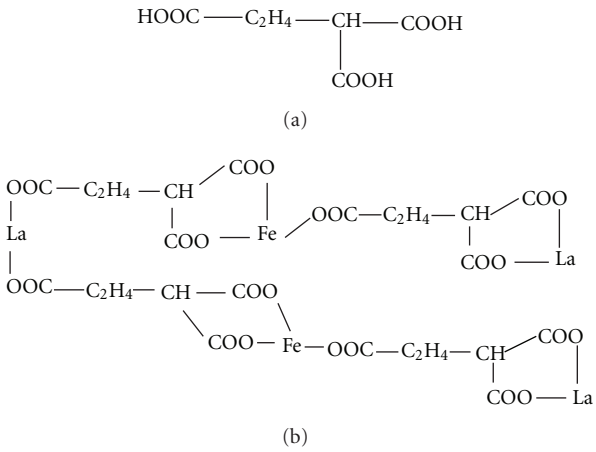

Figure 3: Molecular structure for the citric acid (a) and for a possible complex of metal ions and citric acid (b) in gel precursor of $LaFeO_3$ nanoparticles.

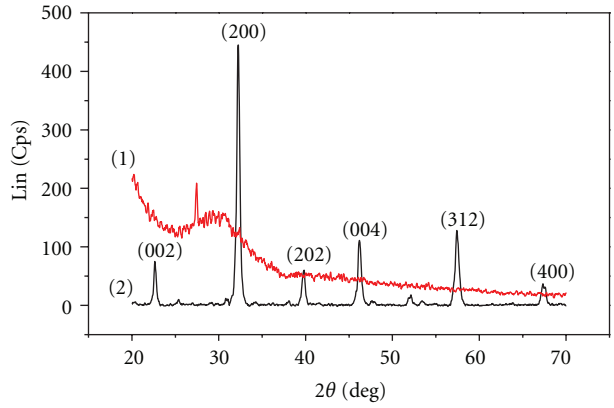

(1) $LaFeO_3$ (500°C, 3 h)

(2) $LaFeO_3$ (500°C, 10 h)

Figure 5: The powder X-ray diffraction patterns of *gel complex* heated at 500°C for 3 hours (red line) and for 10 hours (black line).

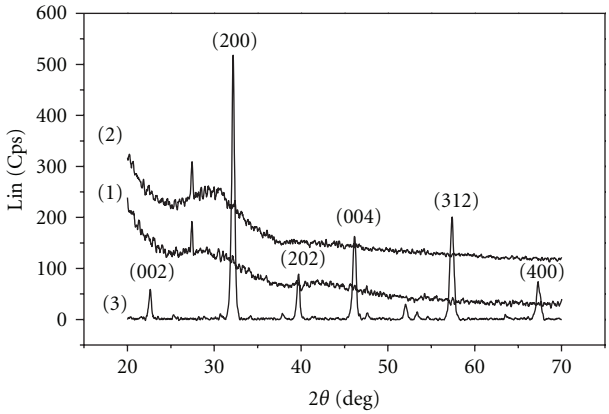

(1) $LaFeO_3$ (300°C)

(2) $LaFeO_3$ (500°C)

(3) $LaFeO_3$ (700°C)

Figure 4: The powder X-ray diffraction patterns of *gel complex* heated at 300°C (line 1); 500°C (line 2); 700°C (line 3) for 3 hours.

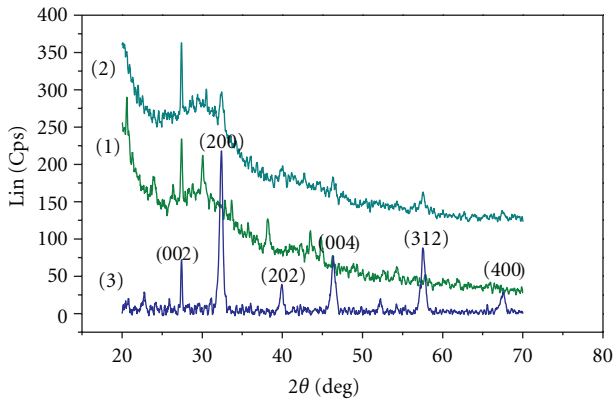

(1) $LaFeO_3$ (300°C)

(2) $LaFeO_3$ (500°C)

(3) $LaFeO_3$ (700°C)

Figure 6: The powder X-ray diffraction patterns of *hydroxide gel* heated at 300°C (line 1); 500°C (line 2); 700°C (line 3) for 3 hours.

it was suggested that the as-prepared gel consists of an intermediate/complex of citric acid, water, and metal ions. On the basis of the above FTIR results, the expected molecular structure of the complex of metal ions and citric acid is shown in Figure 3.

Figure 4 shows the XRD patterns of the nano-sized $LaFeO_3$ powders obtained after heating at different temperatures of 300°C (line 1), 500°C (line 2), and 700°C (line 3) for 3 hours. At 700°C the XRD pattern shows that the major phase is $LaFeO_3$ with orthorhombic crystalline structure. The lattice parameters are $a = 5.546$ Å; $b = 5.5497$ Å; $c = 7.8573$ Å. The gel complex which was heated at 500°C for 3 hours has not yet changed to the $LaFeO_3$ phase, as shown in Figure 4 (line 2) and Figure 5 (red line). It seems to be amorphous, but with further heating at 500°C for 7 hours, the $LaFeO_3$ phase was completely formed (Figure 5—black line). Figure 6 shows the XRD pattern of $LaFeO_3$ prepared by the co-precipitation method. The complex precipitate was heated at different temperatures for 3 hours. The phase states are similar to the case of the sol-gel method (Figure 5). The XRD patterns of hydroxide gel show that the $LaFeO_3$ phase does not appear at 300°C or 500°C; however, at 700°C a major phase as $LaFeO_3$ is formed (Figure 6).

The average crystalline particle size calculated from Scherrer's formula $D = k\lambda/B\cos\theta$ is about 30 nm, where D is the average size of crystalline particle, assuming that particles are spherical, $k = 0.9$ [14], λ is the wavelength of X-ray radiation, B is full width at half maximum of the diffracted peak, and θ is angle of diffraction.

The particle size and morphology of the calcined powders examined by TEM and SEM are shown in Figures 7(a), 7(b), and 8, respectively. It can be estimated from these figures that the particle size is varying from about 10 to 30 nm.

The magnetic properties of the samples were examined by Vibrating Sample Magnetometer (VSM) in the field

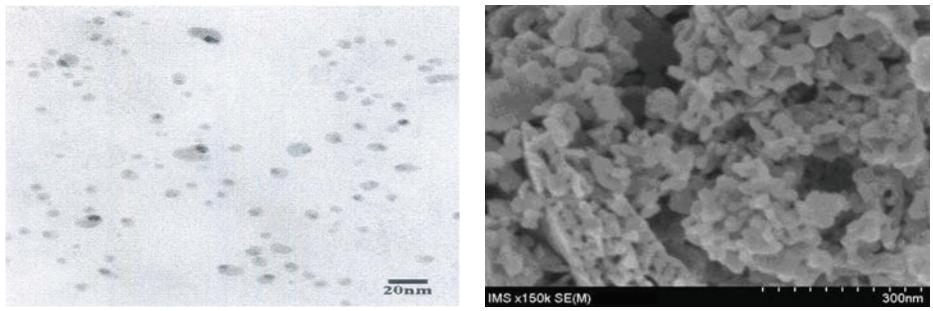

(a) (b)

Figure 7: TEM (a) and SEM (b) micrographs of $LaFeO_3$ prepared by sol-gel method, followed by calcining process at 700°C.

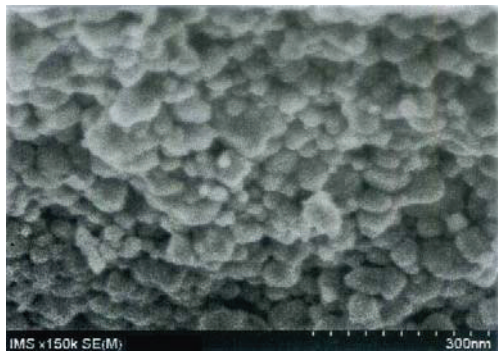

Figure 8: SEM micrograph of nano-$LaFeO_3$ prepared by high-energy milling method.

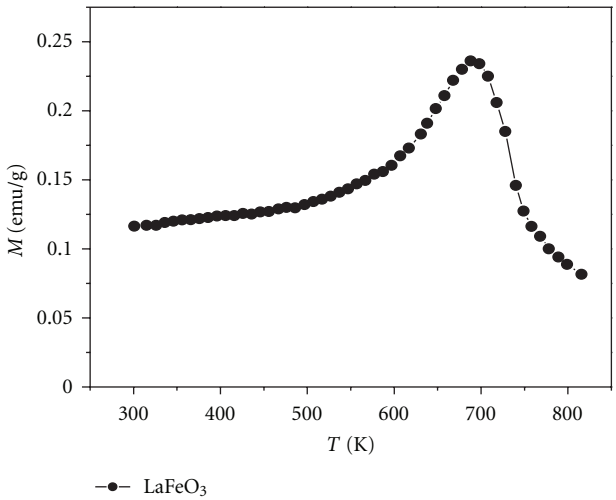

Figure 9: The $M(T)$ curve of nano-$LaFeO_3$ prepared by sol-gel method.

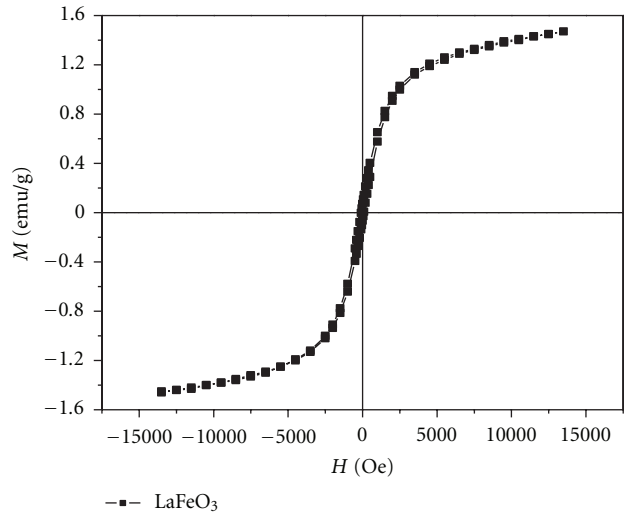

Figure 10: The $M(H)$ curve at room temperature of nano-$LaFeO_3$ prepared by sol-gel method.

of 13.5 kOe from room temperature to 800 K. The Curie temperature determined by the $M(T)$ curve (Figure 9) is around 730 K, which is corresponding to the peak in the DSC curve at about 457°C (Figure 1). The $M(H)$ curve of nano-$LaFeO_3$ prepared by sol-gel method is shown in Figure 10.

As for the sample prepared by high-energy milling the powders after milling were heated at 500°C in 3 hours to eliminate inner stress in the samples. Figure 8 shows the SEM image for the $LaFeO_3$ powder after milling and heat treatment. The average size of particle is about 50 nm. The $M(H)$ curve of nano-sized $LaFeO_3$ prepared by milling method is shown in Figure 11.

It is well known that the perovskite $LaFeO_3$ displays antiferromagnetic and insulator behavior in room temperature [16]. However, the $M(T)$ and $M(H)$ curves of the prepared $LaFeO_3$ show that $LaFeO_3$ exhibits weak ferromagnetism. It may be caused by the antiferromagnetic order with canted spins [17]. In addition, during heating at high temperature some couples of Fe^{3+}-Fe^{2+} may be appeared in $LaFeO_3$ due to the losing of oxygen. The difference between magnetic moment of Fe^{3+} ions (5 μB) and Fe^{2+} (4 μB) has contributed to magnetic behaviors of the samples and they became an electrical conducting materials as semiconductor.

The parameters of hysteresis loop of the samples prepared by sol-gel and milling methods are listed in Table 1.

The results listed in the above table show that the preparation method and particle size influence on the magnetic properties. Although after milling the samples have been

Table 1: The parameters of hysteresis loop of the samples prepared by sol-gel and milling methods.

Parameters	Sol-gel method (Particle size of 30 nm)	Milling method (Particle size of 50 nm)
M_m (emu/g) at $H = 13.5$ kOe	1.464	0.443
M_r (emu/g)	0.078	0.063
H_c (Oe)	92.6	198.9
$S = M_r/M_m$	0.05	0.14

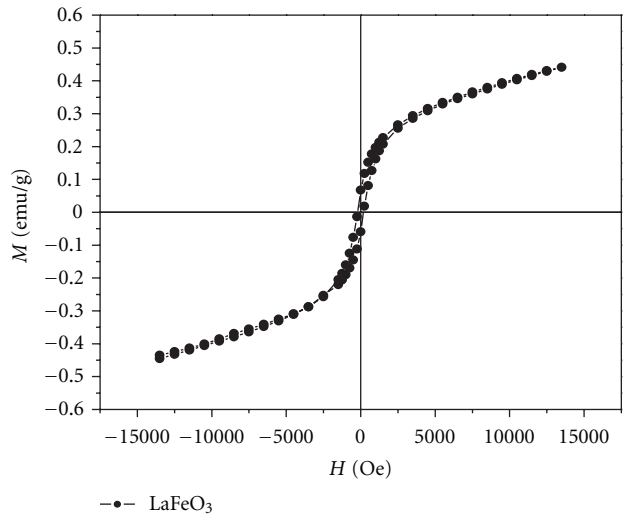

Figure 11: The $M(H)$ curve at room temperature of nano-$LaFeO_3$ prepared by high-energy milling method.

annealed, it seems that the inner press could not be eliminated completely; thus the magnetization M_m of the sample prepared by milling method is less than that of the samples prepared by sol-gel method. The particle size of the powders prepared by the milling method is larger than the one obtained by the sol-gel method. The bigger particles give a higher coercivity H_c. This is in good agreement with the law ($H_c \sim D^6$) of the nanomagnetic particles [18, 19]. It is noted that the nanosized, and single-domain ferromagnetic powder could be superparamagnetic with $H_c = 0$ and $M_r = 0$; $S = (M_r/M_s) = 0$ [20]. If the prepared nano-sized powder has some of particles with multiple domain sizes, H_c, M_r, and S will differ from zero. The larger particle size gives higher S and the ferromagnetic behavior is more clear. That is why we suggested that the ratio $S = M_r/M_s$ could be used as a functionally parameter for evaluating the homogeneity on dimension of nanoparticles and the limit of single domain size of the magnetic nano-sized powder materials.

As mentioned above, the prepared nano-sized $LaFeO_3$ powder is weakly ferromagnetic ($M_r \neq 0$). It is a multidisperse system consisting of the single-domain and multiple-domain particles. The magnetization of the sample is considered as the sum of two terms:

$$M(H) = M^{sp}(H) + M^f(H), \tag{2}$$

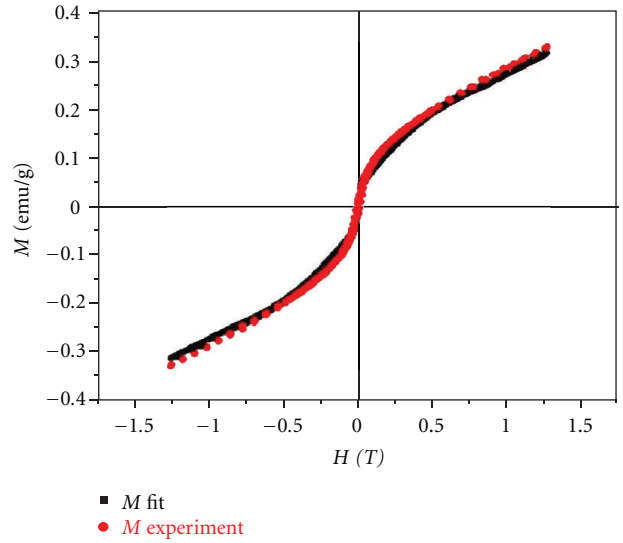

Figure 12: The result of the fitting of the $M(H)$ curve of the nano-$LaFeO_3$ prepared by sol-gel method based on the Langevin function.

where $M^{sp}(H)$ is the contribution from the superparamagnetic (sp) nanoparticles (single domain), $M^f(H)$ is the contribution of ferromagnetic (f) nanoparticles (multiple domains):

$$M^f(H) = \frac{2M_s^f}{\pi}\tan^{-1}\left[\frac{H \pm H_c}{H_c}\tan\left(\frac{\pi S}{2}\right)\right], \tag{3}$$

M_s^f: saturation magnetization of ferromagnetic phase ($M_s^f = M_r/0.866$). S: rectangular coefficence of ferromagetic hysteresis loop.

The noninteraction magnetization process of the superparamagnetic monodisperse nanoparticles can be shown by the expression:

$$M(H) = M(\infty)L\left[\frac{mH}{k_BT}\right], \tag{4}$$

where m is magnetic moment and $L(x) = \coth(x) - 1/x$ is the Langevin function, $x = mH/k_BT$, [21]. To take into account the effects of size dispersion that are always presented in any real system, the magnetization of superparamagnetic particles, in this case, it is better to use the expression:

$$M^{sp}(H) = M^{sp}(\infty)\sum_j f(m_j)L\left[\frac{m_jH}{k_BT}\right]. \tag{5}$$

m_j is magnetic moment of the particle, $f(m_j)$ is weighted terms in Langevin functions [22].

It is suggested that the particles are spherical shape, the distribution of particle size $f(D)$ is shown by the expression [23]:

$$f(D) = \frac{1}{\sqrt{2\pi}\sigma D}\exp\left(-\frac{\ln(D/\overline{D})^2}{2\sigma^2}\right), \tag{6}$$

where σ is standard deviation and $\overline{D}$ is the average particle size. $f(m_j)$ can be calculated from D. Figure 12 shows

the Langevin function fitting result for the magnetization curve of the nano-sized $LaFeO_3$.

4. Conclusion

The nano-sized $LaFeO_3$ has been successfully prepared by different methods. The particle size of nano-$LaFeO_3$ is varying from about 10 to 50 nm depending on the preparation method. The prepared nano-$LaFeO_3$ exhibited a ferromagnetic behavior and the particle size influences the magnetic properties of nano-$LaFeO_3$. The $M(H)$ curve was well fitted by Langevin function. We have proposed that by using parameter $S = M_r/M_s$ one could evaluate the homogeneity of the dimensions of nanoparticles and the critical size of single domain of the nano-magnetic materials.

Acknowledgment

This work was supported by Vietnam's National Foundation For Science and Technology Development (NAFOSTED), with the project code "103.03.69.09".

References

[1] V. Caignaert, A. Maignan, and B. Raveau, "Up to 50 000 per cent resistance variation in magnetoresistive polycrystalline perovskites $Ln_{2/3}Sr_{1/3}MnO_3$ (Ln=Nd; Sm)," *Solid State Communications*, vol. 95, no. 6, pp. 357–359, 1995.

[2] N. Gayathri, A. K. Raychaudhuri, and S. K. Tiwary, "Electrical transport, magnetism, and magnetoresistance in ferromagnetic oxides with mixed exchange interactions: a study of the $La_{0.7}Ca_{0.3}Mn_{1-x}Co_xO_3$ system," *Physical Review B*, vol. 56, pp. 1345–1353, 1997.

[3] H. Taguchi, M. Nagao, and M. Shimada, "Mechanism of metal-insulator transition in the systems $(Ln_{1-x}Ca_x)MnO_{3-\delta}$ (Ln: La, Nd, and Gd) and $(Nd_{0.1}Ca_{0.9-y}Sr_y)MnO_{2.97}$," *Journal of Solid State Chemistry*, vol. 97, no. 2, pp. 476–480, 1992.

[4] Md. A. Choudhury, S. Akhter, D. L. Minh, N. D. Tho, and N. Chau, "Large magnetic-entropy change above room temperature in the colossal magnetoresistance $La_{0.7}Sr_{0.3}Mn_{1-x}Ni_xO_3$ materials," *Journal of Magnetism and Magnetic Materials*, vol. 272, pp. 1295–1297, 2004.

[5] K. Iwasaki, T. Ito, M. Yoshino, T. Matsui, T. Nagasaki, and Y. Arita, "Power factor of $La_{1-x}Sr_xFeO_3$ and $LaFe_{1-y}Ni_yO_3$," *Journal of Alloys and Compounds*, vol. 430, no. 1-2, pp. 297–301, 2007.

[6] M.-H. Hung, M. V. M. Rao, and D.-S. Tsai, "Microstructures and electrical properties of calcium substituted $LaFeO_3$ as SOFC cathode," *Materials Chemistry and Physics*, vol. 101, pp. 297–302, 2007.

[7] D. Bayraktar, F. Clemens, S. Diethelm, T. Graule, J. Van herle, and P. Holtappels, "Production and properties of substituted $LaFeO_3$-perovskite tubular membranes for partial oxidation of methane to syngas," *Journal of the European Ceramic Society*, vol. 27, no. 6, pp. 2455–2461, 2007.

[8] K. Iwasaki, T. Ito, M. Yoshino et al., "Power factor of $La_{1-x}Sr_xFeO_3$ and $LaFe_{1-y}Ni_yO_3$," *Journal of Alloys and Compounds*, vol. 430, pp. 297–301, 2007.

[9] P. Dinka and A. S. Mukasyan, "Perovskite catalysts for the auto-reforming of sulfur containing fuels," *Journal of Power Sources*, vol. 167, no. 2, pp. 472–481, 2007.

[10] M. Yang, A. Xu, and H. Du, "Removal of salicylic acid on perovskite-type oxide $LaFeO_3$ catalyst in catalytic wet air oxidation process," *Journal of Hazardous Materials B*, vol. 139, pp. 86–92, 2007.

[11] X. P. Dai, R. J. Li, C. C. Yu, and Z. P. Hao, "Unsteady-state direct partial oxidation of methane to synthesis gas in a fixed-bed reactor using $AFeO_3$ (A = La, Nd, Eu) perovskite-type oxides as oxygen storage," *Journal of Physical Chemistry B*, vol. 110, no. 45, pp. 22525–22531, 2006.

[12] M. Søgaard, P. V. Hendriksen, and M. Mogensen, "Oxygen nonstoichiometry and transport properties of strontium substituted lanthanum ferrite," *Journal of Solid State Chemistry*, vol. 180, no. 4, pp. 1489–1503, 2007.

[13] A. D. Jadhav, A. B. Gaikwad, V. Samuel, and V. Ravi, "A low temperature route to prepare $LaFeO_3$ and $LaCoO_3$," *Materials Letters*, vol. 61, no. 10, pp. 2030–2032, 2007.

[14] G. Shabbir, A. H. Qureshi, and K. Saeed, "Nano-crystalline $LaFeO_3$ powders synthesized by the citrate-gel method," *Materials Letters*, vol. 60, pp. 3706–3709, 2006.

[15] M. Srivastava, S. Chaubey, and A. K. Ojha, "Investigation on size dependent structural and magnetic behavior of nickel ferrite nanoparticles prepared by sol-gel and hydrothermal methods," *Materials Chemistry and Physics*, vol. 118, no. 1, pp. 174–180, 2009.

[16] S. Komine and E. Iguchi, "Dielectric properties in $LaFe_{0.5}$ $Ga_{0.5}$ O_3 ," *Journal of Physics and Chemistry of Solids*, vol. 68, no. 8, pp. 1504–1507, 2007.

[17] A. V. Galubkov, E. V. Goncharova, V. P. Zhuze, and I. G. Manilove, "Transport mechanism in samarium sulfide," *Soviet Physics Solid State*, vol. 7, no. 8, pp. 1963–1967, 1966.

[18] G. Herzer, "Grain size dependence of coercivity and permeability in nanocrystalline ferromagnets," *IEEE Transactions on Magnetics*, vol. 26, no. 5, pp. 1397–1402, 1990.

[19] D. Xue, G. Chai, X. Li, and X. Fan, "Effects of grain size distribution on coercivity and permeability of ferromagnets," *Journal of Magnetism and Magnetic Materials*, vol. 320, no. 8, pp. 1541–1543, 2008.

[20] J. P. Vejpravova, D. Niznnasky, J. Plocek, A. Hutlova, and J.-L. Rehspringer, "Superparamagnetism of co-ferrite nanoparticles," in *Proceeding of Contributed Paper, Part III (WDS '05)*, pp. 518–523, 2005.

[21] G. F. Goya, T. S. Berquo, and F. C. Fonseca, "Static and dynamic magnetic properties of spherical magnetite nanoparticles," *Journal of Applied Physics*, vol. 94, Article ID 3520, 9 pages, 2003.

[22] F. C. Fonseca, A. S. Ferlauto, F. Alvarez, G. F. Goya, and R. F. Jardim, "Morphological and magnetic properties of carbon-nickel nanocomposite thin films," *Journal of Applied Physics*, vol. 97, Article ID 044313, 7 pages, 2005.

[23] S.-J. Lee, J.-R. Jeong, S.-C. Shin, J.-C. Kim, and J.-D. Kim, "Synthesis and characterization of superparamagnetic maghemite nanoparticles prepared by coprecipitation technique," *Journal of Magnetism and Magnetic Materials*, vol. 282, no. 1–3, pp. 147–150, 2004.